



**HAL**  
open science

## Pharmacological Blockade of Glycoprotein VI Promotes Thrombus Disaggregation in the Absence of Thrombin

Muhammad Usman Ahmed, Valeria Kaneva, Stéphane Loyau, Dmitry Nechipurenko, Nicolas Receveur, Marion Le Bris, Emily Janus-Bell, Mélusine Didelot, Antoine Rauch, Sophie Susen, et al.

► **To cite this version:**

Muhammad Usman Ahmed, Valeria Kaneva, Stéphane Loyau, Dmitry Nechipurenko, Nicolas Receveur, et al.. Pharmacological Blockade of Glycoprotein VI Promotes Thrombus Disaggregation in the Absence of Thrombin. *Arteriosclerosis, Thrombosis, and Vascular Biology*, 2020, 40 (9), pp.2127-2142. 10.1161/ATVBAHA.120.314301 . hal-04376221

**HAL Id: hal-04376221**

**<https://hal.science/hal-04376221v1>**

Submitted on 6 Jan 2024

**HAL** is a multi-disciplinary open access archive for the deposit and dissemination of scientific research documents, whether they are published or not. The documents may come from teaching and research institutions in France or abroad, or from public or private research centers.

L'archive ouverte pluridisciplinaire **HAL**, est destinée au dépôt et à la diffusion de documents scientifiques de niveau recherche, publiés ou non, émanant des établissements d'enseignement et de recherche français ou étrangers, des laboratoires publics ou privés.

# Pharmacological Blockade of Glycoprotein VI Promotes Thrombus Disaggregation in the Absence of Thrombin

Muhammad Usman Ahmed<sup>1</sup>, Valeria Kaneva<sup>2 3 4</sup>, Stéphane Loyau<sup>5</sup>, Dmitry Nechipurenko<sup>2 3 4</sup>, Nicolas Receveur<sup>1</sup>, Marion Le Bris<sup>1</sup>, Emily Janus-Bell<sup>1</sup>, Mélusine Didelot<sup>6</sup>, Antoine Rauch<sup>6</sup>, Sophie Susen<sup>6</sup>, Nabil Chakfé<sup>7</sup>, François Lanza<sup>1</sup>, Elizabeth E Gardiner<sup>8</sup>, Robert K Andrews<sup>9</sup>, Mikhail Pantelev<sup>2 3 4</sup>, Christian Gachet<sup>1</sup>, Martine Jandrot-Perrus<sup>5 10</sup>, Pierre H Mangin<sup>1</sup>

## Affiliations

<sup>1</sup>From the Université de Strasbourg, INSERM, EFS Grand-Est, BPPS UMR-S1255, FMTS, F-67065 Strasbourg, France (M.U.A., N.R., M.L.B., E.J.-B., F.L., C.G., P.H.M.).

<sup>2</sup>Faculty of Physics, Moscow State University, Russia (V.K., D.N., M.P.).

<sup>3</sup>Federal Research and Clinical Centre of Pediatric Hematology, Oncology and Immunology, Russia (V.K., D.N., M.P.).

<sup>4</sup>Center for Theoretical Problems of Physicochemical Pharmacology, Russia (V.K., D.M., M.P.).

<sup>5</sup>Université de Paris, INSERM, Hôpital Bichat, UMR-S1148, France (S.L., M.J.-P.).

<sup>6</sup>CHU Lille, Université de Lille, INSERM UMR-SU1011-EGID, Institut Pasteur de Lille, France (M.D., A.R., S.S.).

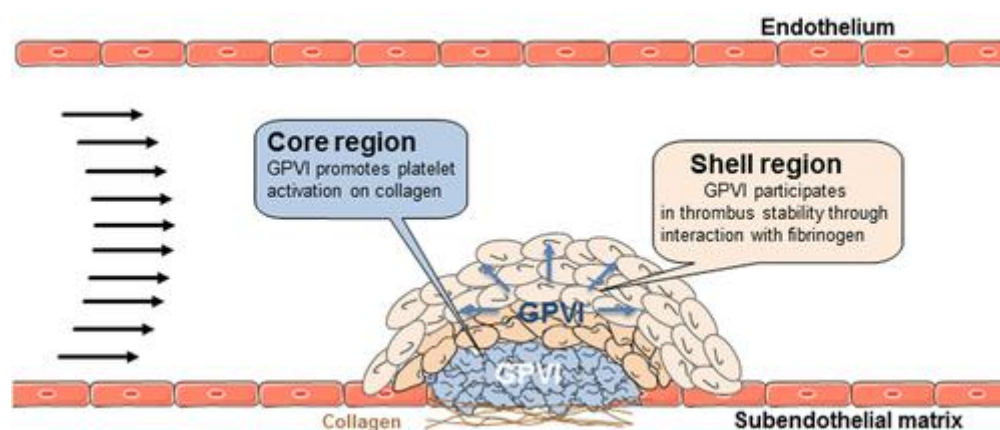
<sup>7</sup>Université de Strasbourg, Department of Vascular Surgery and Kidney Transplantation, France (N.C.).

<sup>8</sup>The Australian National University, The John Curtin School of Medical Research, ACRF Department of Cancer Biology and Therapeutics, Canberra, Australia (E.E.G.).

<sup>9</sup>Australian Centre for Blood Diseases, Monash University, Australia (R.K.A.).

<sup>10</sup>Acticor Biotech, France (M.J.-P.).

## Abstract



**Objective:**

Atherothrombosis occurs upon rupture of an atherosclerotic plaque and leads to the formation of a mural thrombus. Computational fluid dynamics and numerical models indicated that the mechanical stress applied to a thrombus increases dramatically as a thrombus grows, and that strong inter-platelet interactions are essential to maintain its stability. We investigated whether GPVI (glycoprotein VI)-mediated platelet activation helps to maintain thrombus stability by using real-time video-microscopy.

**Approach and Results:**

We showed that GPVI blockade with 2 distinct Fab fragments promoted efficient disaggregation of human thrombi preformed on collagen or on human atherosclerotic plaque material in the absence of thrombin. ACT017-induced disaggregation was achieved under arterial blood flow conditions, and its effect increased with wall shear rate. GPVI regulated platelet activation within a growing thrombus as evidenced by the loss in thrombus contraction when GPVI was blocked, and the absence of the disaggregating effect of an anti-GPVI agent when the thrombi were fully activated with soluble agonists. The GPVI-dependent thrombus stabilizing effect was further supported by the fact that inhibition of any of the 4 key immunoreceptor tyrosine-based motif signalling molecules, src-kinases, Syk, PI3K $\beta$ , or phospholipase C, resulted in kinetics of thrombus disaggregation similar to ACT017. The absence of ACT017-induced disaggregation of thrombi from 2 afibrinogenemic patients suggests that the role of GPVI requires interaction with fibrinogen. Finally, platelet disaggregation of fibrin-rich thrombi was also promoted by ACT017 in combination with r-tPA (recombinant tissue plasminogen activator).

**Conclusions:**

This work identifies an unrecognized role for GPVI in maintaining thrombus stability and suggests that targeting GPVI could dissolve platelet aggregates with a poor fibrin content.

**Highlights**

1. GPVI-mediated platelet activation is important to maintain the stability of a thrombus.
2. Blocking anti-GPVI Fab fragments, but not dimeric GPVI-Fc, promote platelet disaggregation in a shear-dependent manner.
3. The use of anti-GPVI agents which directly target GPVI could promote disaggregation of platelet rich thrombi

## Introduction

Platelets play a central role in hemostasis and in arterial thrombosis. Upon vascular injury platelets adhere, become activated and aggregate to form a hemostatic plug in a healthy vessel and a mural thrombus that can become occlusive, in a diseased artery.<sup>1</sup> It has been reported that the thrombus is heterogeneous in composition with (1) a core, rich in fibrin composed of highly activated platelets located close to the site of injury, in which important amounts of thrombin are generated; (2) a shell, in which platelets are less activated and no significant amounts of thrombin are generated, as evidenced by the absence of fibrin.<sup>2</sup> From a therapeutic point of view, preventing the shell to grow or dissolving it appear as attractive strategies to prevent arterial occlusion and ischemic pathologies.

Platelets express a repertoire of adhesion receptors that engage with subendothelial adhesive matrix proteins after vessel wall injury. Under conditions of elevated blood flow found in arteries, the first step of platelet attachment is initiated by the GP (glycoprotein) Ib-IX-V complex interaction with VWF (von Willebrand factor) present in the subendothelium. Stable adhesion is supported by integrins of the  $\beta 1$  and  $\beta 3$  family, namely  $\alpha 2\beta 1$ ,  $\alpha 5\beta 1$ ,  $\alpha 6\beta 1$ ,  $\alpha \text{IIb}\beta 3$ , and  $\alpha \text{v}\beta 3$  which bind to collagen, fibronectin, laminins, fibrinogen, and vitronectin, respectively. Concomitantly, these receptors together with the collagen receptor, GPVI (glycoprotein VI) initiate intracellular signals leading to platelet activation.<sup>3</sup> Activated platelets release soluble mediators, including thromboxane (Tx)A<sub>2</sub> and ADP which reinforce platelet activation and increase the affinity of integrin  $\alpha \text{IIb}\beta 3$ , for its main ligand, fibrinogen, allowing platelet aggregation.<sup>4</sup> The thrombus composition is heterogeneous with a core containing highly activated platelets and a shell with weakly and reversibly activated platelets.<sup>2</sup> The specific signaling mechanisms responsible for maintenance of platelets in this state is unclear, potential candidates include GPIb (glycoprotein Ib)-dependent signalling,<sup>5</sup> soluble agonists,<sup>2,6</sup> and we recently proposed GPVI.<sup>7</sup>

GPVI is a member of immunoglobulin receptor family which is specifically expressed on megakaryocytes and platelets.<sup>3</sup> GPVI is considered as not being critical for hemostasis, based on the fact that GPVI-deficient subjects present a mild bleeding phenotype and GPVI-deficient mice show no spontaneous bleeding and no prolongation in tail-bleeding time.<sup>8-10</sup> In contrast, it has been reported that absence of GPVI impairs experimental thrombosis in several models of localized vascular injury.<sup>11,12</sup> Remarkably, GPVI-immunodepleted mice were also protected from thrombosis after ultrasound or mechanical injuries to atherosclerotic plaques in ApoE-deficient mice.<sup>13,14</sup> Together, these observations suggest that GPVI is a particularly promising and potentially safe antithrombotic target.<sup>3</sup>

GPVI physically associates with the FcR(Fc receptor)  $\gamma$ -chain and the Src family kinases Lyn and Fyn.<sup>15</sup> Ligand binding to GPVI promotes its clustering which results in phosphorylation of the immunoreceptor tyrosine-based motif of the FcR  $\gamma$ -chain by Src family kinases.<sup>16</sup> This leads to the recruitment of Syk and formation of signaling complexes which activate PLC $\gamma$ 2 (phospholipase C $\gamma$ 2) resulting in mobilization of intracellular Ca<sup>2+</sup> stores, a key second messenger of platelets. GPVI engagement efficiently results in the release of soluble agonists such as ADP and TxA2 which enhance platelet activation.<sup>17</sup> GPVI is best recognized as a platelet activation receptor for fibrillar collagen and supports efficient platelet aggregation in vitro.<sup>17</sup> We and others provided evidence that GPVI participates in platelet activation to laminins.<sup>18,19</sup> We also reported that GPVI plays an important role in platelet adhesion and activation on fibrin.<sup>20,21</sup> More recently, we proposed that human GPVI participates in platelet activation on immobilized fibrinogen, which could support a new role for GPVI in thrombus growth.<sup>7</sup> The primary aim of this study was to investigate the role of GPVI beyond the well-documented initial stages, on the process of thrombus stability. The outcome of this study was to assess the potential of targeting this receptor in the setting of a treatment, when a thrombus had already formed.

We showed that growing thrombi experience elevated mechanical stress, which represents a major challenge to maintain their stability. We developed a numerical model which highlighted the importance of maintaining strong inter-platelet bonds to resist to the increase in mechanical stress when a thrombus grows. Using an experimental approach, we identified a key role of GPVI-mediated platelet activation in maintaining thrombus stability in the absence of thrombin, through its interplay with fibrinogen. These results indicate that targeting GPVI when a platelet-rich aggregate had already formed promotes disaggregation, opening new avenues for the use of anti-GPVI agents to prevent vessel occlusion. In addition, an anti-GPVI agent can also be combined to a thrombolytic agent to dissolve a fibrin-rich thrombus.

## **Materials and Methods**

### **Patients**

Two White patients suffering from congenital afibrinogenemia were collected for the study. The patients were related and expressed the same homozygous mutation c.1001 G>A in exon 5, resulting in a nonsense p.W334X mutation of FGA (fibrinogen A) gene, previously reported to lead to premature termination of translation of fibrinogen  $\alpha$  chain.<sup>22</sup> For these 2 patients, plasma fibrinogen was undetectable by antigen and functional assays with unclottable prothrombin, activated partial thromboplastin, thrombin time, and reptilase time tests. Both patients suffered from spontaneous and post-traumatic bleeds but also had a past

history of arterial or venous thromboembolism (ischemic stroke in patient 1, 2 episodes of superficial venous thrombosis, and 1 episode of deep venous thrombosis in patient 2; the 3 venous thrombosis events in patient 2 occurred under replacement therapy with fibrinogen concentrate) as reported previously.<sup>23</sup> At the time of the study, the 2 patients were treated on demand with fibrinogen concentrates. No infusion of fibrinogen concentrate was performed in the previous 21 days before blood collection. The collection was approved by the French government under the number: DC-2008-642.

### **Computational Fluid Dynamics and Fluid-Structure Interaction Analysis**

To assess the evolution of mechanical stress during thrombus growth, we used computational fluid dynamics combined with additional fluid-structure interaction analysis. Thrombi were represented as the hemi-spheres protruding into vessels of 600  $\mu\text{m}$  diameter. Constant pressure boundary conditions were chosen for the blood flow corresponding to a wall shear rate (WSR) of  $300 \text{ s}^{-1}$ . Subendothelial matrix and thrombus were represented as isotropic elastic media with Young modulus value derived from thrombus nanoindentation analysis,<sup>24</sup> while blood was considered as a Newtonian fluid. A fluid-structure interaction module of Comsol Multiphysics was used for computation of flow and flow-induced mechanical stress throughout the system. See Figure I and Table I in the Data Supplement for more details.

### **Computational Model of Thrombus Formation**

We developed a 2-dimensional model of thrombus formation with platelets represented by particles of different sizes.<sup>25</sup> The model considers 2 types of inter-platelet interaction: (1) a primary GPIb-VWF-mediated interaction, modelled by stochastically associating and disassociating springs between platelets; the model was validated using experiments addressing platelet interactions with VWF-coated surfaces<sup>26</sup>; (2) an  $\alpha\text{IIb}\beta\text{3}$ -fibrinogen-mediated interaction modelled by Morse potential. Parameters of potential were acquired using experimental data on forces between single platelets.<sup>27</sup> The adhesive force increases with the time platelets spend in the thrombus. To study thrombus dynamics during the initial phase of thrombus growth, we decreased integrin-mediated force between platelets by 10% to 80%. Blood was considered as an incompressible Newtonian fluid described with Navier-Stokes and the continuity equations. The flow field was computed considering the partial vessel blockade by the thrombus. Equations describing both the flow profile and hydrodynamical forces that act on platelets were solved using the Open-FOAM (field operation and manipulation) simpleFoam solver.<sup>28</sup> To infer how inter-platelet forces depend on both thrombus size and shear rate, the stationary configuration of tightly (hexagonally)

packed equally sized disks under steady flow was analyzed. Disks, which represented platelets, were gathered in a semi-spherically shaped thrombus. To simplify the analysis, only Morse potential was used to describe platelet-platelet attraction. Injury was modelled as the array of adhesive interaction sites localized at the vessel wall.

### **In Vitro Flow-Based Adhesion Assay**

Microfluidic flow chambers or glass microslides (for scanning electron microscopy experiments) were prepared as previously described.<sup>29</sup> For most experiments, human hirudinized blood (100 U/mL) was perfused through the microfluidic channels, with the exception of flows on plaque material for which we used nonrecalcified citrated blood. The human atherosclerotic plaque homogenates (1 mg/mL) prepared as previously described.<sup>30</sup> To form fibrin-rich clots, citrated blood incubated with DIOC<sub>6</sub> (0.5 μmol/L) to label platelets and with DyLight 650-conjugated anti-fibrin (10 μg/mL) was recalcified with CaCl<sub>2</sub> (12.5 mmol/L) and MgCl<sub>2</sub> (3.5 mmol/L) immediately before perfusing it through collagen coated microfluidic chambers at 1500 s<sup>-1</sup>. Disaggregation of a thrombus was defined as the detachment of at least 3 platelets or more in a field.

### **Light Transmission Aggregometry**

Human washed platelets were prepared from ACD-anticoagulated blood by sequential centrifugation as previously described.<sup>31</sup> The platelets were suspended at a concentration of 3×10<sup>5</sup>/μL in Tyrode buffer containing 0.35% human serum albumin and 2 μL/mL apyrase. Platelet aggregation was measured turbidimetrically after addition of different agonists, in the presence of human fibrinogen (0.8 mg/mL).

### **Scanning Electron Microscopy**

Adherent platelets in glass microslides were fixed for 45 minutes with 25 mg/mL glutaraldehyde in 0.1 mol/L cacodylate buffer containing 20 mg/mL sucrose (305 mOsm, pH 7.3) and scanning electron microscopy was performed as previously described.<sup>5</sup>

### **Statistical Analysis**

Results are expressed as mean±SEM. All statistical analyses were performed with the GraphPad Prism program, version 5.0 (Prism, GraphPad, LaJolla, CA). Nonparametric Mann-Whitney *U* test was used when applicable, and  $\chi^2$  test with CI of 95% was used for categorical variables. One-way ANOVA or 2-way ANOVA followed with a post hoc Bonferroni was used for multiple comparisons. *P*<0.05 were considered statistically significant. Details are found in the figure legends.

## **Results**

### **Blood Flow-Induced Mechanical Stress Challenges the Stability of a Growing Thrombus**

A mural thrombus in an injured artery experiences forces applied by the flowing blood. Computational fluid dynamics simulations indicated that surface shear stress was maximal at the thrombus apex and increases with thrombus height (Figure 1A through 1C). These external stress acting on the surface is redistributed throughout the thrombus and results in internal mechanical stress. Fluid-structure interaction analysis performed using the continuous 3-dimensional model indicated that internal mechanical stress (von Mises stress) was maximal at the thrombus base and was also increased with both thrombus height and blood flow velocities (Figure I in the Data Supplement). Similar results were obtained in a particle-based 2-dimensional model showing that inter-platelet forces within a thrombus were maximal at its base reaching elevated values of 350 pN for a thrombus of 26  $\mu\text{m}$  in height and increased with thrombus height and WSR (Figure 1D through 1F). Together, these results indicate that both flow-dependent surface forces and internal platelet-platelet forces increase as a mural thrombus is growing in the vessel lumen. To assess the impact of flow-induced mechanical forces during thrombus growth, we developed a numerical particle-based model of thrombus formation dynamics which reproduces rheology found in arteries ( $750 \text{ s}^{-1}$ ). This model recapitulates the main features of thrombosis with (1) platelet adhesion, (2) platelet activation depicted as they become darker (various levels of activation ranging from white (resting) to grey (activated)), and (3) recruitment of circulating platelets which results in linear thrombus growth (Figure 1G and 1H; Movie I in the Data Supplement). The impact of elevated shear on thrombus stability was evidenced by the disruption of the thrombus occurring when a 3-fold increase in shear rate was applied at 30 seconds, (Figure 1I; Movie II in the Data Supplement). The importance of the inter-platelet bond strength in maintaining thrombus stability was shown by disaggregation taking place when the inter-platelet force was reduced by 40% at 30 seconds (Figure 1J; Movie III in the Data Supplement). This disaggregation highlighted the importance of a sustained platelet activation during thrombus growth to maintain its integrity. As GPVI is an activation receptor, we investigated whether it participates in maintaining thrombus ability to resist mechanical stress and whether its targeting could promote disaggregation.

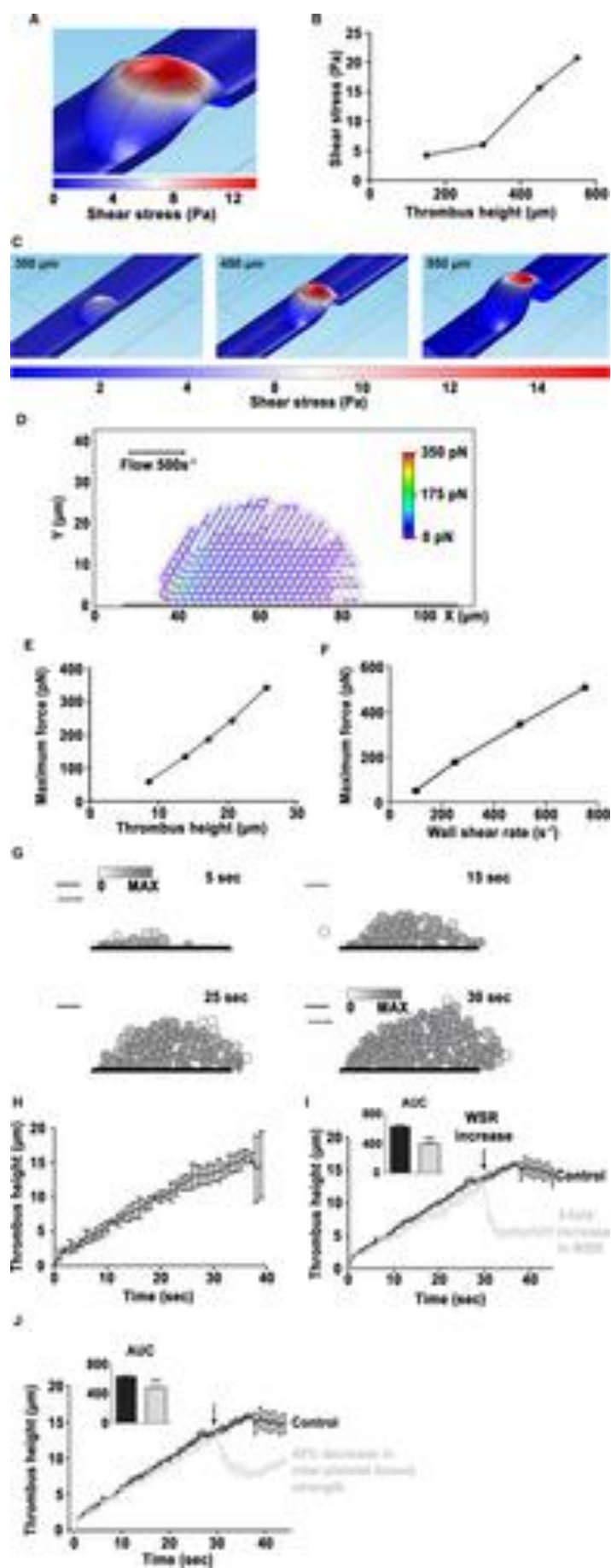


**Figure 1. In silico evidence that sustained platelet activation is crucial for the stability of a growing thrombus.** **A–C**, Computational fluid dynamics simulations were performed to determine surface shear stress exerted on a semi-spherical thrombi of different sizes. **A**, Image representing the distribution of the shear stress on the surface of thrombi of 450  $\mu\text{m}$  at flow conditions corresponding to wall shear rates of  $300\text{ s}^{-1}$  (at sites distal to thrombus). **B**, Point-connecting line graph represents the shear stress as a function of thrombus height at constant pressure drop boundary conditions. **C**, Images represent the distribution of the shear stress on the surface of thrombi of 300  $\mu\text{m}$ , 450  $\mu\text{m}$ , and 550  $\mu\text{m}$  height in a channel of 600  $\mu\text{m}$  at constant pressure drop boundary conditions. **D**, Distribution of inter-platelet forces in a 2-dimensional (2D) thrombus subjected to the flow corresponding to  $500\text{ s}^{-1}$ . Each inter-platelet force is shown as a line colored corresponding to the force value. Only forces corresponding to extended inter-platelet bonds are shown. Platelets contours are shown in gray color. **E**, The dependence of maximum inter-platelet bond extension force on thrombus height obtained in a 2D model (wall shear rate [WSR] of  $500\text{ s}^{-1}$ ). **F**, The dependence of maximum inter-platelet bond extension force on a wall shear rate obtained for 2D thrombus of 26  $\mu\text{m}$  height. **G**, Representative images of the dynamics of thrombus formation in silico. The injury region is shown in black; platelets are represented by circles of different colors (darkening color reflects the extent of platelet activation). WSR is  $750\text{ s}^{-1}$ ; arrow indicates flow direction. Scale bar represents 5  $\mu\text{m}$ . **H–J**, The graphs plot thrombus height over time at  $750\text{ s}^{-1}$ . **I**, The arrow represents the time at which a 3-fold increase in WSR was applied (**H** and **I**;  $n=6$ ). **J**, The arrow represents the time at which the force between platelets was reduced by 40% ( $n=10$ ). Bar graph represents area under curve (AUC). Nonparametric Mann-Whitney  $U$  Test;  $***P<0.001$ .

### **Blockade of GPVI During Thrombus Growth Promotes Disaggregation in the Absence of Thrombin**

Hirudinated human whole blood was flowed over collagen to preform aggregates followed by perfusion of 50  $\mu\text{g/mL}$  of a blocking humanized anti-GPVI Fab fragment, ACT017, at an arterial WSR of  $750\text{ s}^{-1}$ . Real-time video-microscopy showed that numerous individual platelets detached from the top of aggregates treated with ACT017 resulting in a clear disaggregation (Figure 2A; Movie IV in the Data Supplement). Quantification indicated a 4.9-fold increase in the number of platelet thrombi disaggregating after treatment with ACT017 when compared with control buffer (Figure 2B). ACT017 also lowered the time to initiation of disaggregation by 45% (Figure 2C). The diaggregating effect of ACT017 was also

evidenced when we maintained whole blood perfusion throughout the experiment (Movie V in the Data Supplement) and was not limited to hirudin as an anticoagulant, as a similar result was obtained with heparin and citrate (data not shown). Similar results were obtained on human atherosclerotic plaque material, where ACT017 promoted efficient disaggregation of platelet thrombi that were formed with citrated blood (Figure 2D). This disaggregation obtained by blocking GPVI was not restricted to ACT017, as another GPVI blocker, the Fab fragment of 1G5 mAb exhibited similar effects (Figure 2E). In contrast, thrombi did not disaggregate when equivalent concentrations of Fab fragments of the nonblocking anti-GPVI antibody 3J24 were perfused, suggesting that the inhibitory effect of ACT017 and 1G5 is related to their ability to disrupt ligand binding to GPVI (Figure 2F and 2G). Finally, we observed that soluble GPVI-Fc, used at a concentration which inhibits collagen-induced platelet aggregation, did not disaggregate preformed aggregates (Figure 2F and 2G). Together, these results indicate that direct blockade of GPVI ligand binding, but not a competition approach, promotes disaggregation of preformed platelet thrombi, highlighting a novel role of GPVI in maintaining the stability of a thrombus during its build-up when thrombin generation was blocked. In the rest of our study, we have mainly used ACT017 as an agent that directly blocks GPVI.

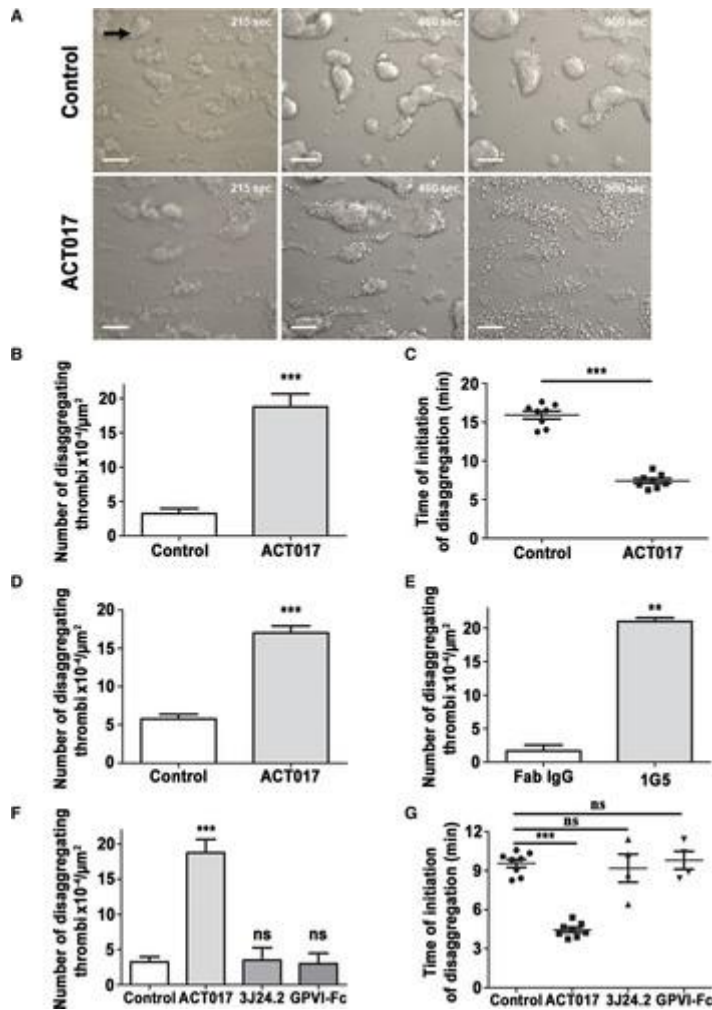


**Figure 2. GPVI (glycoprotein VI) blockade promotes disaggregation of preformed thrombi in vitro.** **A–C** and **E–G**, Hirudinized (100 U/mL) human whole blood was perfused for 3 min at  $750 \text{ s}^{-1}$  through microfluidic flow chambers coated with a solution of type I fibrillar collagen (200  $\mu\text{g}/\text{mL}$ ) to preform aggregates. **A–C**, ACT017 (50  $\mu\text{g}/\text{mL}$ ) or control buffer was perfused over the preformed aggregates at  $750 \text{ s}^{-1}$  for 12 min. **A**, Representative differential interference contrast microscopy images of thrombi subjected to ACT017 or control buffer diluted in PBS. The black arrow indicates the flow direction. Scale bars represent 20  $\mu\text{m}$ . **B**, Bar graphs represent the number of disaggregating thrombi ( $\times 10^{-4}/\mu\text{m}^2$ ); control:  $3.2 \times 10^{-4} \pm 0.7 \times 10^{-4}$  disaggregating thrombi/ $\mu\text{m}^2$ ; ACT017:  $18.7 \times 10^{-4} \pm 1.9 \times 10^{-4}$  disaggregating thrombi/ $\mu\text{m}^2$ ; \*\*\* $P < 0.001$ ,  $n = 8$ . **C**, Scatter plots represent the time at which disaggregation was initiated, expressed in minutes; mean  $\pm$  SEM; nonparametric Mann-Whitney  $U$  Test; control:  $9.6 \pm 0.3$  min; ACT017:  $4.4 \pm 0.1$  min; \*\*\* $P < 0.001$ ,  $n = 8$  (**D**) Citrated (3.2%) human whole blood was perfused for 4 min at  $300 \text{ s}^{-1}$  through glass microslides coated with a solution of human atherosclerotic plaque

homogenates (1 mg/mL) to preform aggregates, before perfusing ACT017 (50  $\mu\text{g/mL}$ ) or control buffer in the same blood at  $300\text{ s}^{-1}$  for 12 min. Bar graphs represent the number of disaggregating thrombi ( $\times 10^{-4}$ )/ $\mu\text{m}^2$  ( $n=4$ ). mean $\pm$ SEM; nonparametric Mann-Whitney *U* Test; \*\*\* $P<0.001$ . **E**, 1G5 (50  $\mu\text{g/mL}$ ) or Fab IgG diluted in PBS was perfused over preform aggregates at  $750\text{ s}^{-1}$  for 12 min. Bar graphs represent the number of disaggregating thrombi ( $\times 10^{-4}$ )/ $\mu\text{m}^2$  ( $n=3$ ). Two-tailed paired *t* test; \*\* $P<0.01$ . **F**, ACT017 (50  $\mu\text{g/mL}$ ), 3J24.2 (50  $\mu\text{g/mL}$ ), GPVI-Fc (50  $\mu\text{g/mL}$ ), or control buffer diluted in PBS were perfused over the preformed aggregates at  $750\text{ s}^{-1}$  for 12 min. Bar graphs represent the number of disaggregating thrombi ( $\times 10^{-4}$ )/ $\mu\text{m}^2$ ; control:  $3.7\times 10^{-4}\pm 0.9\times 10^{-4}$  disaggregating thrombi/ $\mu\text{m}^2$ ; 3J24.2:  $3.5\times 10^{-4}\pm 1.7\times 10^{-4}$  disaggregating thrombi/ $\mu\text{m}^2$ ; ns,  $P>0.5$ ,  $n=4-8$ . **G**, Scatter plots represent time to initiation of disaggregation, expressed in minutes;  $3.0\times 10^{-4}\pm 1.4\times 10^{-4}$  disaggregating thrombi/ $\mu\text{m}^2$ ; non significant (ns);  $P>0.5$ ,  $n=4-8$ . Bar is the mean $\pm$ SEM; Bonferroni multiple comparison test; \*\*\* $P<0.001$ .

### **Shear Forces Promote Disaggregation of Platelet Aggregates When GPVI Is Blocked**

We next evaluated whether ACT017 promotes disaggregation in a Born-type aggregometer. Washed human platelets were stimulated with collagen, U46619 or ADP, and ACT017 was added to the suspension once aggregation reached maximal values. We did not observe any disaggregation upon the addition of ACT017 (Figure 3A). Because shear is low in an aggregometer ( $<100\text{ s}^{-1}$ ), one hypothesis could be that ACT017-induced platelet disaggregation occurring in the blood perfusion assay depends on the presence of elevated shear forces. To examine that, we preformed aggregates in the flow system at  $750\text{ s}^{-1}$  for 3 minutes and perfused ACT017 at WSR ranging from  $150\text{ s}^{-1}$  up to  $750\text{ s}^{-1}$ . In agreement with the result obtained in the light transmission aggregometer, ACT017 did not promote disaggregation of platelet thrombi under venous blood flow conditions ( $150\text{ s}^{-1}$ ), (Figure 3B). In contrast, signs of disaggregation were observed at an arterial WSR of  $300\text{ s}^{-1}$  with a maximal number of disaggregating thrombi being achieved at  $750\text{ s}^{-1}$  (Figure 3B and 3C). Measuring the initial time of thrombus disaggregation further highlighted the importance of increasing blood flow conditions on ACT017-induced platelet thrombus disaggregation (Figure 3D). These results are in agreement with our observations *in silico* showing that elevated shear forces promote disaggregation when platelet activation is inhibited.

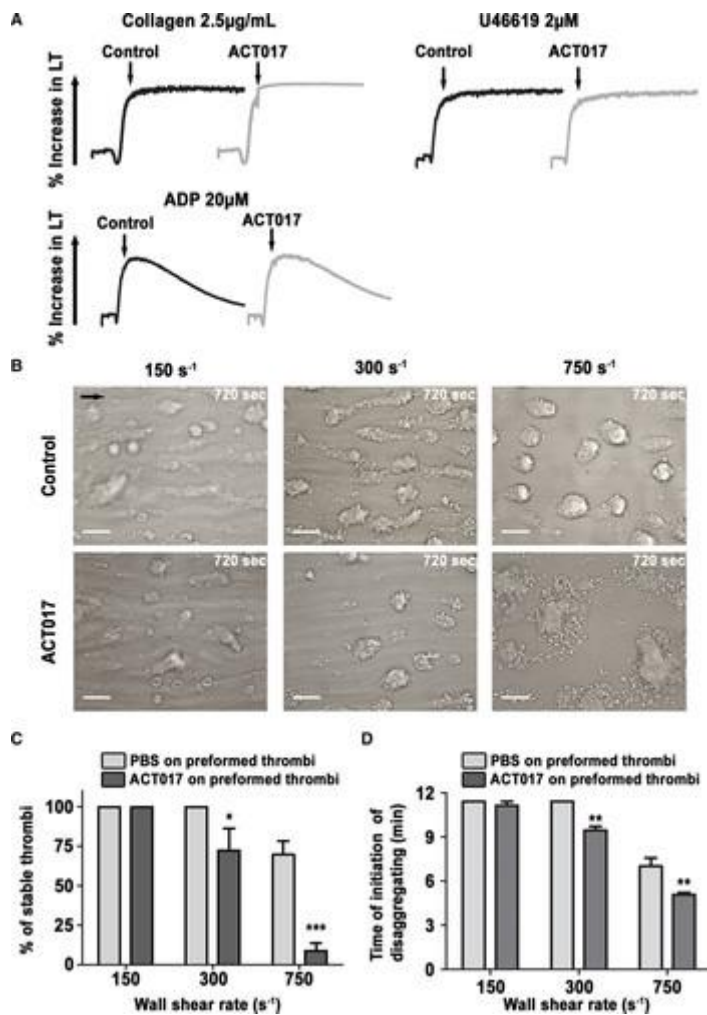


**Figure 3. Shear regulates ACT017-induced disaggregation of preformed thrombi.** **A**, Human washed platelets ( $3.0 \times 10^5/\mu\text{L}$ ) were stimulated with collagen ( $2.5 \mu\text{g/mL}$ ), U46619 ( $2 \mu\text{mol/L}$ ) or ADP ( $20 \mu\text{mol/L}$ ) in the presence of fibrinogen ( $64 \mu\text{g/mL}$ ). ACT017 ( $50 \mu\text{g/mL}$ ) or control buffer was added at maximal aggregation (indicated by an arrow). Aggregation profiles are representative of 3 separate experiments ( $n=3$ ). **B–D**, Hirudinated ( $100 \text{ U/mL}$ ) human whole blood was perfused over immobilized collagen ( $200 \mu\text{g/mL}$ ) for 3 min at  $750 \text{ s}^{-1}$  to preform aggregates. Then, ACT017 ( $50 \mu\text{g/mL}$ ) diluted in PBS was perfused over preformed aggregates at different wall shear rate (WSR;  $150 \text{ s}^{-1}$ ,  $300 \text{ s}^{-1}$ , and  $750 \text{ s}^{-1}$ ) for 12 min. **B**, Representative differential interference contrast microscopy images of thrombi subjected to ACT017 or control buffer diluted in PBS at indicated WSR. The black arrow indicates the flow direction. Scale bars represent  $20 \mu\text{m}$ . **C**, Bar graph represents the percentage of stable thrombi ( $n=3$ ).  $\chi^2$  test with CI of 95%; \* $P < 0.05$  and \*\*\* $P < 0.001$ . **D**, Interleaved bars represent time to initiation of disaggregation after perfusion of ACT017 or

control buffer diluted in PBS over human aggregates, expressed in minutes (n=3); mean±SEM. Bonferroni multiple comparison test; \*\*\* $P<0.001$ .

### **The Disaggregating Effect of GPVI Blockade Relies on the Inhibition of Platelet Activation**

As GPVI is an activation receptor, we hypothesized that ACT017-induced disaggregation in the absence of thrombin, is linked to an impairment of GPVI-mediated platelet activation in the growing thrombus. To test this hypothesis, we perfused elevated nonphysiological concentrations of soluble agonists (ADP or TRAP [thrombin receptor activator peptide]) over preformed aggregates to maximally activate platelets and overcome the GPVI activatory pathway, before injecting ACT017. We observed that under such conditions ACT017 was less efficient in promoting disaggregation and that the time of disaggregation was delayed, indicating that its effect is linked to the regulation of platelet activation (Figure 4A and 4B). In parallel, we examined thrombus contraction in real-time, as a readout of platelet activation. While thrombi were contracting and appeared more compact over time in the control, a clear loosening and surface expansion was observed when ACT017 was perfused over contracted thrombi (Figure 4C; Movie VI in the Data Supplement). This was confirmed by quantification which showed that the surface occupied by the ACT017-treated thrombi was significantly increased in comparison with untreated control (Figure 4D). Scanning electron microscopy images confirmed the loosening of the aggregates treated with ACT017 and showed that individual platelets were also less contracted when compared with control, confirming that ACT017 impairs platelet activation (Figure 4E). As GPVI promotes platelet activation through a signaling pathway that has been well characterized, we evaluated the effect of inhibitors of several key immunoreceptor tyrosine-based motif signaling proteins such as src-kinase (PP2), Syk (PRT060318), PI3K $\beta$  (phosphoinositide 3-kinase; TGX-221), and PLC $\gamma$ 2 (U73122). The inhibitors increased the number of disaggregating thrombi by 3.6-fold, 2.6-fold, 2.2-fold, and 4.4-fold, respectively, to a similar level as the once achieved with ACT017 (Figure 4F). Moreover, the initial time of thrombus disaggregation also showed a significant decrease for all 4 inhibitors when compared with control which was very close to the one of ACT017 (Figure 4G). The number of disaggregating thrombi and time of initiation of disaggregation were very similar between ACT017 and 1G5 (Figure 2) as compared with inhibition of the 4 immunoreceptor tyrosine-based motif signaling molecules, suggesting that disaggregation occurring when GPVI is blocked, relies on an impairment of GPVI-mediated platelet activation.

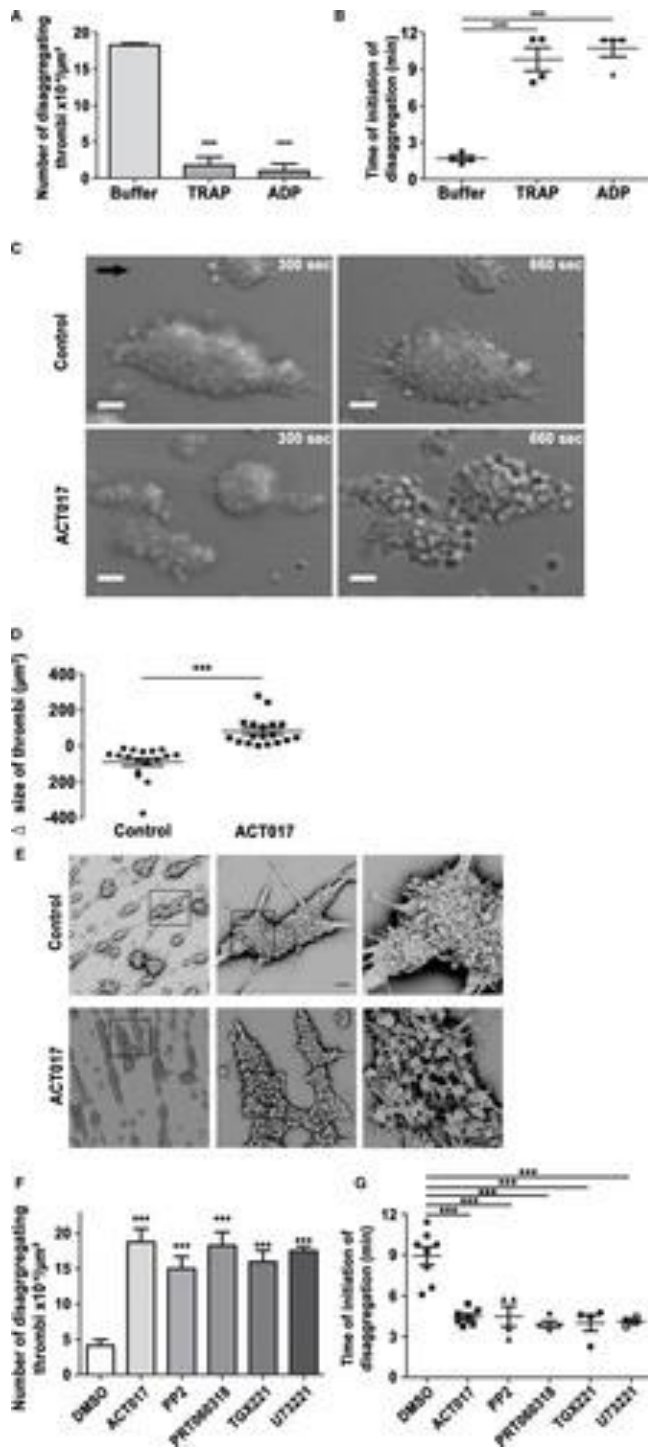


**Figure 4. The disaggregating effect of ACT017 relies on impairment of GPVI (glycoprotein VI)-mediated platelet activation.** A–B, Hirudinized (100 U/mL) human whole blood was perfused for 3 min at 750 s<sup>-1</sup> through microfluidic flow chambers coated with a solution of type I fibrillar collagen (200 μg/mL) to preform aggregates, before perfusing buffer containing or not ADP (50 μmol/L) or TRAP (thrombin receptor activator peptide; 50 μmol/L) at 750 s<sup>-1</sup> for 2 min and then at 150 s<sup>-1</sup> for 3 min, followed by ACT017 (50 μg/mL) or control buffer diluted in PBS at 750 s<sup>-1</sup> for 12 min. **A**, Bar graphs represent the number of

disaggregating thrombi ( $\times 10^{-4}$ )/ $\mu\text{m}^2$  (n=4). **B**, Scatter plot represents the time at which disaggregation was initiated, expressed in minutes (n=4). mean $\pm$ SEM; Bonferroni multiple comparison test; \*\*\* $P < 0.001$ . **C–D**, Hirudinated (100 U/mL) human whole blood was perfused for 3 min at  $750 \text{ s}^{-1}$  through microfluidic flow chambers coated with a solution of type I fibrillar collagen (200  $\mu\text{g}/\text{mL}$ ) to preform aggregates, before perfusing ACT017 (50  $\mu\text{g}/\text{mL}$ ) or control buffer diluted in PBS at  $750 \text{ s}^{-1}$  for 12 min. **C**, Representative differential interference contrast microscopy images of thrombi subjected to ACT017 or control buffer at 5 and 11 min. The black arrow indicates the flow direction. Scale bars represent 5  $\mu\text{m}$ . **D**, Scatter plot represents the variation in thrombi size measured between 5 and 11 min (n=3). Mean $\pm$ SEM; nonparametric Mann-Whitney *U* test;  $\Delta$ size: control:  $-90.2 \pm 20.7 \mu\text{m}^2$ ; ACT017:  $82.0 \pm 18.3 \mu\text{m}^2$ ; \*\*\* $P < 0.001$ ; n=3. **E**, Representative scanning electron microscopy images of thrombi subjected to ACT017 or control buffer at 15 min. Scale bars represent 5  $\mu\text{m}$ . **F–G**, Hirudinated (100 U/mL) human whole blood was perfused for 3 min at  $750 \text{ s}^{-1}$  through microfluidic flow chambers coated with a solution of type I fibrillar collagen (200  $\mu\text{g}/\text{mL}$ ) to preform aggregates, before perfusing ACT017 (50  $\mu\text{g}/\text{mL}$ ), PP2 (5  $\mu\text{mol}/\text{L}$ ), PRT060318 (5  $\mu\text{mol}/\text{L}$ ), TGX-221 (1  $\mu\text{mol}/\text{L}$ ), and U73122 (5  $\mu\text{mol}/\text{L}$ ) or DMSO diluted in PBS at  $750 \text{ s}^{-1}$  for 12 min. **F**, Bar graphs represent the number of disaggregating thrombi ( $\times 10^{-4}$ )/ $\mu\text{m}^2$ ; control:  $4.1 \times 10^{-4} \pm 0.8 \times 10^{-4}$  disaggregating thrombi/ $\mu\text{m}^2$ ; ACT017:  $18.7 \times 10^{-4} \pm 1.9 \times 10^{-4}$  disaggregating thrombi/ $\mu\text{m}^2$ ; PP2:  $15 \times 10^{-4} \pm 1.7 \times 10^{-4}$  disaggregating thrombi/ $\mu\text{m}^2$ ; PRT060318:  $18.2 \times 10^{-4} \pm 1.9 \times 10^{-4}$  disaggregating thrombi/ $\mu\text{m}^2$ ; TGX-221:  $16 \times 10^{-4} \pm 1.5 \times 10^{-4}$  disaggregating thrombi/ $\mu\text{m}^2$ ; U73122:  $17.5 \times 10^{-4} \pm 0.6 \times 10^{-4}$  disaggregating thrombi/ $\mu\text{m}^2$ ; \*\*\* $P < 0.001$ ; n=4–8. **G**, Scatter plot represents the time at which disaggregation was initiated, expressed in minutes (n=4–8). Mean $\pm$ SEM; Bonferroni multiple comparison test; control:  $8.9 \pm 0.6$  min; PP2:  $4.5 \pm 0.7$  min; PRT060318:  $3.8 \pm 0.2$  min; TGX-221:  $4.0 \pm 0.5$  min; U73122:  $4.1 \pm 0.1$  min; \*\*\* $P < 0.001$ ; n=4; \*\*\* $P < 0.001$ .

### **Disaggregation Induced When GPVI Is Blocked Relies on the Presence of Fibrinogen**

We recently proposed that the role of GPVI in thrombus build-up relies on its ability to promote platelet activation on fibrinogen.<sup>7</sup> To evaluate whether thrombus disaggregation occurring when GPVI is blocked, is linked to this property, we performed experiments with blood of 2 patients with congenital afibrinogenemia. We observed that perfusion of hirudinated whole blood of both patients over immobilized collagen resulted in the formation of thrombi at  $750 \text{ s}^{-1}$ , even though they appeared smaller than the control (Figure 5A). This was expected since platelet aggregation in the absence of significant levels of fibrinogen has been previously reported and shown to rely on VWF.<sup>32</sup> While ACT017-induced thrombus

disaggregation in the control, little effect was observed on thrombi of either patient at  $750 \text{ s}^{-1}$  (Figure 5B). This result indicates that blockade of GPVI has no impact on thrombus disaggregation in the absence of normal levels of fibrinogen, even though these thrombi appeared looser than normal thrombi in agreement with a previous report.<sup>33</sup> Quantification confirmed the absence of ACT017-induced disaggregation with blood from the patients as compared with controls (Figure 5C). These results propose the existence of a link between fibrinogen and GPVI in allowing the stability of a growing thrombus.

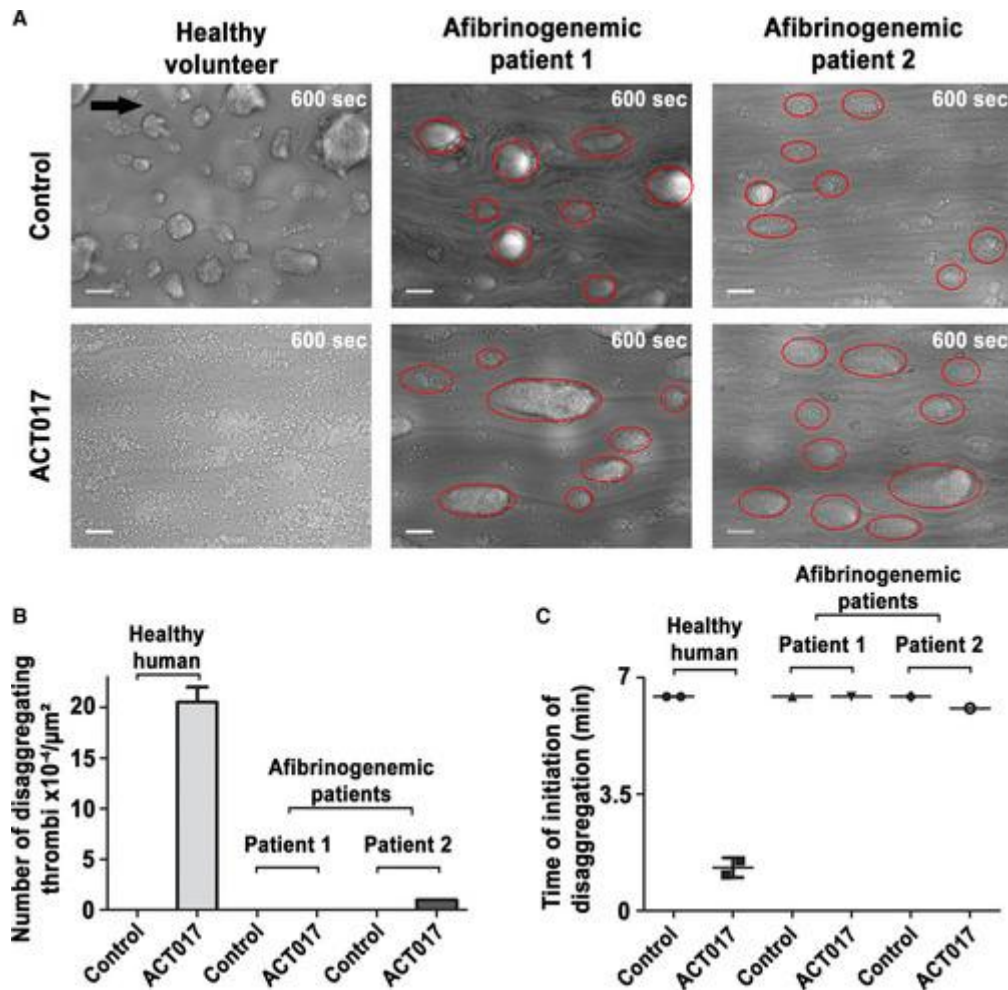


**Figure 5. ACT017-induced thrombus disaggregation depends on fibrinogen.** Hirudinized (100 U/mL) human whole blood from healthy volunteers or patients suffering from afibrinogenemia was perfused for 3 min at  $750 \text{ s}^{-1}$  through microfluidic flow chambers coated with a solution of type I fibrillar collagen (200  $\mu\text{g}/\text{mL}$ ) to preform aggregates, before perfusing blood containing ACT017 (50  $\mu\text{g}/\text{mL}$ ) or control buffer for 7 min. **A**, Representative differential interference contrast microscopy images of thrombi subjected to ACT017 or control buffer. The black arrow indicates the flow direction. Scale bars represent 20  $\mu\text{m}$ . **B**, Bar graphs represent the number of disaggregating thrombi ( $\times 10^{-4}/\mu\text{m}^2$ ) ( $n=2$ ). **C**, Scatter plots represent the time at which disaggregation was initiated,

expressed in minutes; ACT017: healthy human:  $20.5 \times 10^{-4} \pm 1.5 \times 10^{-4}$  disaggregating thrombi/ $\mu\text{m}^2$ ; afibrinogenemic patient-1 and 2:  $0.0 \times 10^{-4} \pm 0.0 \times 10^{-4}$  disaggregating thrombi/ $\mu\text{m}^2$ ; (n=2).

### **Combination of ACT017 and r-tPA Promotes Disaggregation of Fibrin-Rich Clots In Vitro**

So far, we observed that GPVI contributes to the stabilization of a platelet-rich thrombus which contains no fibrin, suggesting that anti-GPVI agents could remove the part of the thrombus corresponding to the shell.<sup>34</sup> We next evaluated whether blockade of GPVI has also an impact on a thrombus core in which thrombin is found and which is stabilized by fibrin. Initially, we formed fibrin-rich thrombi by perfusing recalcified citrated human blood over collagen at  $1500 \text{ s}^{-1}$ . The high fibrin content of the thrombi was evidenced on 3-dimensional reconstructed images obtained with a fluorescently conjugated anti-fibrin antibody (Figure 6A). ACT017 had a minor effect on thrombus disaggregation with detaching platelets being mainly localized at the thrombus edge where less fibrin was present, which is explained by the ability of fibrin to entrap platelets and thereby stabilize the thrombus (Figure 6B; Movie VII in the Data Supplement). This result is in agreement with the view that fibrin stabilizes the clot. We next wondered whether ACT017 would cooperate with a thrombolytic approach based on r-tPA (recombinant tissue plasminogen activator) to enhance thrombus disaggregation. We showed that perfusion of r-tPA in platelet-poor plasma efficiently reduced the fibrin signal over time confirming its thrombolytic effect (Figure 6C and 6D). We observed that r-tPA alone promoted thrombus disaggregation which was probably linked to its ability to lyse fibrin and lower the stability of the thrombus (Figure 6E). Interestingly, combining r-tPA with ACT017 significantly increased thrombus disaggregation as compared with r-tPA alone, highlighting the potential of an anti-GPVI agent combined with a thrombolytic reagent to promote thrombus disaggregation (Figure 6E). Similar results were obtained when a combination of ACT017 and r-tPA was perfused over thrombi formed on a tissue factor-collagen coated surface with a clear loosening of platelet aggregates being evidenced by a marked increase in surface occupied by the thrombi (Figure 6F and 6G). Together, these results suggest that combining a thrombolytic strategy with a blockade of GPVI could dissolve mural thrombi lodged in the vascular bed.

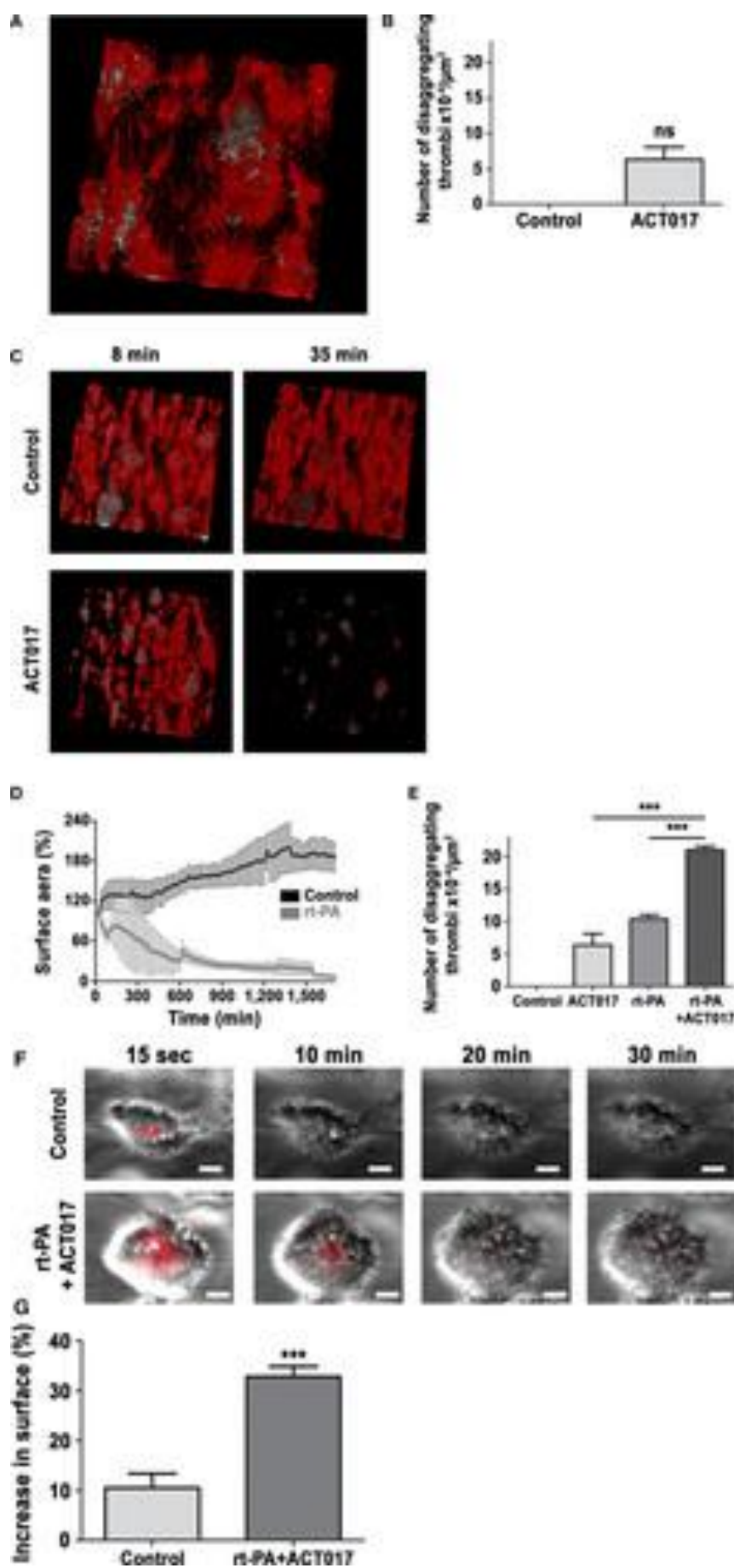


**Figure 6. Effect of ACT017 and r-tPA (recombinant tissue plasminogen activator) on disaggregation of fibrin-rich clots.** Citrated (3.2%) human whole blood was labelled with a DyLight 650-coupled anti-fibrin antibody (10  $\mu\text{g}/\text{mL}$ ) and was recalcified by adding  $\text{CaCl}_2$  (12.5  $\text{mmol}/\text{L}$ ) and  $\text{MgCl}_2$  (3.5  $\text{mmol}/\text{L}$ ) just before perfusing it through collagen coated microfluidic flow chambers at  $1500 \text{ s}^{-1}$ . Once platelet-rich thrombi were formed, a brief washing step was performed to rinse the thrombi before perfusing platelet-poor plasma (PPP) obtained from the same donor (hirudinized blood) in the presence of ACT017 (50  $\mu\text{g}/\text{mL}$ ) or r-tPA (50  $\mu\text{g}/\text{mL}$ ) alone or in combination, at  $3000 \text{ s}^{-1}$  for 35 min. **A**, Representative 3-dimensional (3D) reconstructed confocal microscopy image of thrombi. Fibrin is stained in red and platelets in gray. **B**, Bar graphs represent the number of disaggregating thrombi ( $\times 10^{-4}/\mu\text{m}^2$ ) ( $n=3$ ). Mean $\pm$ SEM; nonparametric Mann-Whitney  $U$  test; ns denotes not significant. **C**, Representative 3D reconstructed confocal microscopy image of thrombi subjected to r-tPA or control buffer diluted in PPP. **D**, Connecting line graphs represent the surface area coverage of fibrin (expressed as percentage of control) over time ( $n=3$ ); mean $\pm$ SEM. **E**, Bar graphs represent the number of disaggregating thrombi ( $\times 10^{-4}/\mu\text{m}^2$ ) ( $n=3$ ). Mean $\pm$ SEM; Bonferroni multiple comparison test; \*\*\* $P<0.001$ . **F** and **G**, Citrated (3.2%) human whole blood was labelled with a DyLight 650-coupled anti-fibrin antibody (10  $\mu\text{g}/\text{mL}$ ) and was recalcified by adding  $\text{CaCl}_2$  (12.5  $\text{mmol}/\text{L}$ ) and  $\text{MgCl}_2$  (3.5  $\text{mmol}/\text{L}$ ) just before perfusing it through collagen and TF-coated microfluidic flow chambers at  $1500 \text{ s}^{-1}$ . **F**, Representative bright field/epifluorescence microscopy images of r-tPA pretreated thrombi subjected to ACT017 or control buffer diluted in PPP. Fibrin appears in red. **G**, Bar graphs represent increase in surface occupied (expressed in percentage) by the disaggregating thrombi ( $n=3$ ). Mean $\pm$ SEM;  $\chi^2$  test with CI of 95%; control:  $10.5\pm 2.9\%$  increase in surface area; ACT017:  $32.5\pm 2.0\%$  increase in surface area \*\*\* $P<0.01$ ;  $n=3$ .

## Discussion

In this study, based on the in silico model of thrombus dynamics, we propose that under conditions of arterial blood flow, thrombus dynamics is sensitive to platelet activation state which determines the critical platelet-platelet forces within the thrombus. A decrease in platelet activation level or an increase in the blood flow, result in platelet disaggregation in the numerical model. This in silico result is perfectly in line with the disaggregating effect of ACT017 observed in vitro, which is expected to lower platelet activation state within the thrombi and with the fact that this disaggregating effect increases with the higher values of blood flow (WSR). This study demonstrates that platelet activation is not a short-lived process

which aims only to activate integrins to allow bond formation, but represents a long-lasting process that maintains strong inter-platelet bonds.

Most of the experiments performed in this study have been based on perfusions of anticoagulated blood in flow chambers which represents a limitation, as no thrombin is generated under such conditions and, therefore, differs from an *in vivo* situation. On the contrary, such a situation could mimic the part of the thrombus named the shell, in which it has been reported that no significant amount of thrombin is found based on the absence of fibrin.

We have recently reported that blockade of GPVI impairs the growth of a thrombus that had already formed most likely by preventing platelet activation and, therefore, aggregation.<sup>7</sup> We proposed that this effect was linked to an inhibition of GPVI/fibrinogen-mediated platelet activation, as platelets from GPVI-deficient patients were unable to spread on fibrinogen. The importance of GPVI/fibrinogen interaction in thrombus formation is further evidenced in the present article through the use of blood from afibrinogenemic patients. First, we confirmed that perfusing fibrinogen-poor blood over collagen formed thrombi, through a mechanism proposed to rely on VWF/ $\alpha$ IIB $\beta$ 3 interaction.<sup>32</sup> We observed that while ACT017-induced disaggregation of control thrombi, it had little effect on thrombi formed with blood from 2 afibrinogenemic patients. Importantly, ACT017 exhibited almost no effect despite the fact that such thrombi were looser than control and, therefore, more prone to disaggregate.<sup>33</sup> This result suggests that the effect of GPVI blockade on thrombus disaggregation could be linked to its interplay with fibrinogen. Moreover, observation of thrombus disaggregation in real-time clearly shows that platelets detaching are the one on the top of the thrombus, that is, those interacting with fibrinogen, and never those attached to the surface through strong interaction with collagen.

It is well accepted that absence or blockade of GPVI prevents thrombus formation *in vitro* and in several *in vivo* models of experimental thrombosis.<sup>11,12</sup> These results underscore a potential beneficial role of anti-GPVI agents in preventing arterial thrombosis, notably during percutaneous coronary intervention. Indeed, this procedure leads to exposure of highly reactive fibrillar collagen which initiates platelet activation and thrombus formation through GPVI. Therefore, blocking GPVI in such a setting now stands as a very promising antithrombotic strategy. Anti-GPVI agents could also be beneficial in patients with an ongoing thrombosis in addition to their use in prevention since we recently reported that an anti-GPVI blocking agent, ACT017, limits thrombus growth once a thrombus had already formed.<sup>7</sup> The results presented in this article extend these findings, showing that anti-GPVI

agents promote disaggregation of thrombi, which was unexpected. This disaggregating effect was observed on fibrin-poor thrombi, which mimic the thrombus shell, representing the prominent part of the thrombus. This suggests that anti-GPVI agents could destabilize the shell, thereby preventing vessel occlusion. Additionally, we showed that thrombi rich in fibrin, a condition that mimics the core of the thrombus, are also destabilized by ACT017 when used in combination with r-tPA. The disaggregating effects of anti-GPVI agents used in combination with r-tPA on fibrin-rich thrombi opens new avenues for the use of such agents in clinical settings where a thrombus had already formed, such as during acute phases of myocardial infarction or stroke. This adds new arguments to previous observations that mice immunodepleted for GPVI were protected in a stroke model, in favor of a beneficial effect of anti-GPVI antibodies in stroke.<sup>35</sup>

This study presented the results obtained exclusively from experiments *in vitro* with human blood. In this model, human whole blood is perfused over fibrillar collagen and forms a mural thrombus which is likely to mimic a pathological situation encountered during arterial thrombosis. We aimed to confirm these observations *in vivo*. As ACT017 blocks human but not mouse GPVI, we used a mouse strain in which murine GPVI was genetically replaced by its human counterpart.<sup>36</sup> To our surprise, ACT017 did not promote disaggregation of preformed mouse platelet thrombi *in vitro*, indicating that GPVI is not important to maintain the integrity of mouse thrombi (article in preparation). For these reasons, evaluating the effect of blocking human GPVI on thrombus stability during the initial phase of thrombus growth could not be achieved in a mouse. This is not the only example of major differences between platelets of the 2 species, other being related to the thrombin receptors and the presence of the immunoreceptor tyrosine-based motif receptor, Fc $\gamma$ RIIa (Fc gamma receptor IIA).

Dimeric GPVI-Fc, unlike the 2 distinct blocking anti-GPVI Fab fragments ACT017 and 1G5, did not promote thrombus disaggregation. There is strong experimental evidence that dimeric GPVI-Fc inhibits collagen-induced platelet aggregation *in vitro* and *ex vivo*. GPVI-Fc also reduces experimental thrombosis probably through impairing GPVI interaction with collagen exposed at site of injury.<sup>37,38</sup> The reason why GPVI-Fc has no effect on thrombus disaggregation could have 2 explanations. First, direct blockade of GPVI with an antibody has been proposed to be more efficient than using a competition approach based on GPVI-Fc in static and flow experiments.<sup>34,35</sup> Second, we reported that dimeric GPVI-Fc does not bind fibrinogen, which is the ligand of GPVI in a growing thrombus,<sup>7</sup> and therefore, it is expected that such an agent would have no effect. This observation has important clinical implications as ACT017 and GPVI-Fc have both successfully completed phase I and are currently being

evaluated in phase II clinical trials.<sup>39,40</sup> Here we describe that direct blockade of GPVI with Fab fragments, but not with GPVI-Fc, promotes disaggregation of both fibrin-poor and fibrin-rich thrombi. Our data suggests that such agents should be evaluated in trials of patients with ischemic stroke treated with r-tPA. This is especially relevant since anti-GPVI agents do not appear to impact hemostasis and so carry a reduced bleeding risk when compared with other antiplatelet agents.<sup>3</sup>

### **Nonstandard Abbreviations and Acronyms**

<b>Fc</b>	<b>Fc receptor</b>
<b>GP</b>	<b>glycoprotein</b>
<b>PI3K</b>	<b>phosphoinositide 3-kinase</b>
<b>r-tPA</b>	<b>recombinant tissue plasminogen activator</b>
<b>VWF</b>	<b>von Willebrand factor</b>
<b>WSR</b>	<b>wall shear rate</b>

### **Acknowledgments**

We thank Wolfgang Siess for providing atherosclerotic plaque material as a control.

### **Sources of Funding**

This work was supported by ARMESA (Association Recherche et Développement Médical en santé publique) and by a grant from Concours mondial de l'innovation: TherAVC 2.0 (BPI France). M.U. Ahmed was supported by PhD fellowship from HEC (Higher Education Commission) Pakistan.

### **Disclosures**

M. Jandrot-Perrus is the founder of Acticor Biotech. C. Gachet is the cofounder of Acticor

Correspondence to: Pierre H Mangin, Université de Strasbourg, INSERM, EFS Grand-Est, BPPS UMR-S1255, FMTS, F-67065 Strasbourg, France. Email pierre.mangin@efs.sante.fr

### **References**

- **1.**Jackson SP. Arterial thrombosis—insidious, unpredictable and deadly.**Nat Med.** 2011; 17:1423–1436. doi: 10.1038/nm.2515
- **2.**Welsh JD, Stalker TJ, Voronov R, Muthard RW, Tomaiuolo M, Diamond SL, Brass LF. A systems approach to hemostasis: 1. The interdependence of thrombus architecture and agonist movements in the gaps between platelets.**Blood.** 2014; 124:1808–1815. doi: 10.1182/blood-2014-01-550335
- **3.**Zahid M, Mangin P, Loyau S, Hechler B, Billiald P, Gachet C, Jandrot-Perrus M. The future of glycoprotein VI as an antithrombotic target.**J Thromb Haemost.** 2012; 10:2418–2427. doi: 10.1111/jth.12009
- **4.**Versteeg HH, Heemskerk JW, Levi M, Reitsma PH. New fundamentals in hemostasis.**Physiol Rev.** 2013; 93:327–358. doi: 10.1152/physrev.00016.2011
- **5.**Mangin P, Yuan Y, Goncalves I, Eckly A, Freund M, Cazenave JP, Gachet C, Jackson SP, Lanza F. Signaling role for phospholipase C gamma 2 in platelet glycoprotein Ib alpha calcium flux and cytoskeletal reorganization. Involvement of a pathway distinct from FcR gamma chain and Fc gamma RIIA.**J Biol Chem.** 2003; 278:32880–32891. doi: 10.1074/jbc.M302333200
- **6.**Gachet C. ADP receptors of platelets and their inhibition.**Thromb Haemost.** 2001; 86:222–232.
- **7.**Mangin PH, Onselaer MB, Receveur N, Le Lay N, Hardy AT, Wilson C, Sanchez X, Loyau S, Dupuis A, Babar AK, et al. Immobilized fibrinogen activates human platelets through glycoprotein VI.**Haematologica.** 2018; 103:898–907. doi: 10.3324/haematol.2017.182972
- **8.**Dumont B, Lasne D, Rothschild C, Bouabdelli M, Ollivier V, Oudin C, Ajzenberg N, Grandchamp B, Jandrot-Perrus M. Absence of collagen-induced platelet activation caused by compound heterozygous GPVI mutations.**Blood.** 2009; 114:1900–1903. doi: 10.1182/blood-2009-03-213504
- **9.**Hermans C, Wittevrongel C, Thys C, Smethurst PA, Van Geet C, Freson K. A compound heterozygous mutation in glycoprotein VI in a patient with a bleeding disorder.**J Thromb Haemost.** 2009; 7:1356–1363. doi: 10.1111/j.1538-7836.2009.03520.x
- **10.**Matus V, Valenzuela G, Sáez CG, Hidalgo P, Lagos M, Aranda E, Panes O, Pereira J, Pillois X, Nurden AT, et al. An adenine insertion in exon 6 of human GP6 generates a truncated protein associated with a bleeding disorder in four Chilean families.**J Thromb Haemost.** 2013; 11:1751–1759. doi: 10.1111/jth.12334
- **11.**Bender M, Hagedorn I, Nieswandt B. Genetic and antibody-induced glycoprotein VI deficiency equally protects mice from mechanically and FeCl(3) -induced thrombosis.**J Thromb Haemost.** 2011; 9:1423–1426. doi: 10.1111/j.1538-7836.2011.04328.x
- **12.**Mangin P, Yap CL, Nonne C, Sturgeon SA, Goncalves I, Yuan Y, Schoenwaelder SM, Wright CE, Lanza F, Jackson SP. Thrombin overcomes the thrombosis defect associated with platelet GPVI/FcRgamma deficiency.**Blood.** 2006; 107:4346–4353. doi: 10.1182/blood-2005-10-4244

- **13.**Hechler B, Nonne C, Eckly A, Magnenat S, Rinckel JY, Denis CV, Freund M, Cazenave JP, Lanza F, Gachet C. Arterial thrombosis: relevance of a model with two levels of severity assessed by histologic, ultrastructural and functional characterization.**J Thromb Haemost.** 2010; 8:173–184. doi: 10.1111/j.1538-7836.2009.03666.x
- **14.**Kuijpers MJ, Gilio K, Reitsma S, Nergiz-Unal R, Prinzen L, Heeneman S, Lutgens E, van Zandvoort MA, Nieswandt B, Egbrink MG, et al. Complementary roles of platelets and coagulation in thrombus formation on plaques acutely ruptured by targeted ultrasound treatment: a novel intravital model.**J Thromb Haemost.** 2009; 7:152–161. doi: 10.1111/j.1538-7836.2008.03186.x
- **15.**Suzuki-Inoue K, Tulasne D, Shen Y, Bori-Sanz T, Inoue O, Jung SM, Moroi M, Andrews RK, Berndt MC, Watson SP. Association of Fyn and Lyn with the proline-rich domain of glycoprotein VI regulates intracellular signaling.**J Biol Chem.** 2002; 277:21561–21566. doi: 10.1074/jbc.M201012200
- **16.**Quek LS, Pasquet JM, Hers I, Cornall R, Knight G, Barnes M, Hibbs ML, Dunn AR, Lowell CA, Watson SP. Fyn and Lyn phosphorylate the Fc receptor gamma chain downstream of glycoprotein VI in murine platelets, and Lyn regulates a novel feedback pathway.**Blood.** 2000; 96:4246–4253.
- **17.**Nieswandt B, Watson SP. Platelet-collagen interaction: is GPVI the central receptor?**Blood.** 2003; 102:449–461. doi: 10.1182/blood-2002-12-3882
- **18.**Inoue O, Suzuki-Inoue K, McCarty OJ, Moroi M, Ruggeri ZM, Kunicki TJ, Ozaki Y, Watson SP. Laminin stimulates spreading of platelets through integrin alpha6beta1-dependent activation of GPVI.**Blood.** 2006; 107:1405–1412. doi: 10.1182/blood-2005-06-2406
- **19.**Schaff M, Tang C, Maurer E, Bourdon C, Receveur N, Eckly A, Hechler B, Arnold C, de Arcangelis A, Nieswandt B, et al. Integrin  $\alpha 6 \beta 1$  is the main receptor for vascular laminins and plays a role in platelet adhesion, activation, and arterial thrombosis.**Circulation.** 2013; 128:541–552. doi: 10.1161/CIRCULATIONAHA.112.000799
- **20.**Alshehri OM, Hughes CE, Montague S, Watson SK, Frampton J, Bender M, Watson SP. Fibrin activates GPVI in human and mouse platelets.**Blood.** 2015; 126:1601–1608. doi: 10.1182/blood-2015-04-641654
- **21.**Mammadova-Bach E, Ollivier V, Loyau S, Schaff M, Dumont B, Favier R, Freyburger G, Latger-Cannard V, Nieswandt B, Gachet C, et al. Platelet glycoprotein VI binds to polymerized fibrin and promotes thrombin generation.**Blood.** 2015; 126:683–691. doi: 10.1182/blood-2015-02-629717
- **22.**Neerman-Arbez M, de Moerloose P, Bridel C, Honsberger A, Schönböerner A, Rossier C, Peerlinck K, Claeysens S, Di Michele D, d’Oiron R, et al. Mutations in the fibrinogen alpha gene account for the majority of cases of congenital afibrinogenemia.**Blood.** 2000; 96:149–152.

- **23.** Simsek I, de Mazancourt P, Horellou MH, Erdem H, Pay S, Dinc A, Samama MM. Afibrinogenemia resulting from homozygous nonsense mutation in A alpha chain gene associated with multiple thrombotic episodes. **Blood Coagul Fibrinolysis**. 2008; 19:247–253. doi: 10.1097/MBC.0b013e3282f564fd
- **24.** Swieringa F, Baaten CC, Verdoold R, Mastenbroek TG, Rijnveld N, van der Laan KO, Breel EJ, Collins PW, Lancé MD, Henskens YM, et al. Platelet control of fibrin distribution and microelasticity in thrombus formation under flow. **Arterioscler Thromb Vasc Biol**. 2016; 36:692–699. doi: 10.1161/ATVBAHA.115.306537
- **25.** Paulus JM. Platelet size in man. **Blood**. 1975; 46:321–336.
- **26.** Coburn LA, Damaraju VS, Dozic S, Eskin SG, Cruz MA, McIntire LV. GPIIb/IIIa-vWF rolling under shear stress shows differences between type 2B and 2M von Willebrand disease. **Biophys J**. 2011; 100:304–312. doi: 10.1016/j.bpj.2010.11.084
- **27.** Nguyen TH, Palankar R, Bui VC, Medvedev N, Greinacher A, Delcea M. Rupture forces among human blood platelets at different degrees of activation. **Sci Rep**. 2016; 6:25402. doi: 10.1038/srep25402
- **28.** Trifanov PV, Kaneva VN, Strijhak SV, Pantelev MA, Ataulakhanov FI, Dunster J, Voevodin VV, Nechipurenko DY. Developing quasi-steady model for studying hemostatic response using supercomputer technologies. **Supercomput Front Innov**. 2018; 5:67–72
- **29.** Maurer E, Schaff M, Receveur N, Bourdon C, Mercier L, Nieswandt B, Dubois C, Jandrot-Perrus M, Goetz JG, Lanza F, et al. Fibrillar cellular fibronectin supports efficient platelet aggregation and procoagulant activity. **Thromb Haemost**. 2015; 114:1175–1188. doi: 10.1160/TH14-11-0958
- **30.** Penz SM, Reininger AJ, Toth O, Deckmyn H, Brandl R, Siess W. Glycoprotein IIb/IIIa inhibition and ADP receptor antagonists, but not aspirin, reduce platelet thrombus formation in flowing blood exposed to atherosclerotic plaques. **Thromb Haemost**. 2007; 97:435–443.
- **31.** Cazenave JP, Ohlmann P, Cassel D, Eckly A, Hechler B, Gachet C. Preparation of washed platelet suspensions from human and rodent blood. **Methods Mol Biol**. 2004; 272:13–28. doi: 10.1385/1-59259-782-3:013
- **32.** De Marco L, Girolami A, Zimmerman TS, Ruggeri ZM. von Willebrand factor interaction with the glycoprotein IIb/IIIa complex. Its role in platelet function as demonstrated in patients with congenital afibrinogenemia. **J Clin Invest**. 1986; 77:1272–1277. doi: 10.1172/JCI112430
- **33.** Remijn JA, Wu YP, Ijsseldijk MJ, Zwaginga JJ, Sixma JJ, de Groot PG. Absence of fibrinogen in afibrinogenemia results in large but loosely packed thrombi under flow conditions. **Thromb Haemost**. 2001; 85:736–742.

- **34.**Jamasbi J, Megens RT, Bianchini M, Münch G, Ungerer M, Faussner A, Sherman S, Walker A, Goyal P, Jung S, et al. Differential inhibition of human atherosclerotic plaque-induced platelet activation by dimeric GPVI-Fc and Anti-GPVI antibodies: functional and imaging studies.**J Am Coll Cardiol.** 2015; 65:2404–2415. doi: 10.1016/j.jacc.2015.03.573
- **35.**Kleinschnitz C, Pozgajova M, Pham M, Bendszus M, Nieswandt B, Stoll G. Targeting platelets in acute experimental stroke: impact of glycoprotein Ib, VI, and IIb/IIIa blockade on infarct size, functional outcome, and intracranial bleeding.**Circulation.** 2007; 115:2323–2330. doi: 10.1161/CIRCULATIONAHA.107.691279
- **36.**Mangin PH, Tang C, Bourdon C, Loyau S, Freund M, Hechler B, Gachet C, Jandrot-Perrus M. A humanized glycoprotein VI (GPVI) mouse model to assess the antithrombotic efficacies of anti-GPVI agents.**J Pharmacol Exp Ther.** 2012; 341:156–163. doi: 10.1124/jpet.111.189050
- **37.**Bültmann A, Herdeg C, Li Z, Münch G, Baumgartner C, Langer H, Kremmer E, Geisler T, May A, Ungerer M, et al. Local delivery of soluble platelet collagen receptor glycoprotein VI inhibits thrombus formation in vivo.**Thromb Haemost.** 2006; 95:763–766.
- **38.**Massberg S, Konrad I, Bültmann A, Schulz C, Münch G, Peluso M, Lorenz M, Schneider S, Besta F, Müller I, et al. Soluble glycoprotein VI dimer inhibits platelet adhesion and aggregation to the injured vessel wall in vivo.**FASEB J.** 2004; 18:397–399. doi: 10.1096/fj.03-0464fje
- **39.**Lebozec K, Jandrot-Perrus M, Avenard G, Favre-Bulle O, Billiald P. Design, development and characterization of ACT017, a humanized Fab that blocks platelet's glycoprotein VI function without causing bleeding risks.**MAbs.** 2017; 9:945–958. doi: 10.1080/19420862.2017.1336592
- **40.**Ungerer M, Rosport K, Bültmann A, Piechatzek R, Uhland K, Schlieper P, Gawaz M, Münch G. Novel antiplatelet drug revacept (Dimeric Glycoprotein VI-Fc) specifically and efficiently inhibited collagen-induced platelet aggregation without affecting general hemostasis in humans.**Circulation.** 2011; 123:1891–1899. doi: 10.1161/CIRCULATIONAHA.110.980623